Image classification of experimental yields for cardiomyocyte cells differentiated from human induced pluripotent stem cells

Samira Mohammadi, Ferdous Finklea, Mohammadjafar Hashemi, Elizabeth Lipke, and Selen Cremaschi*

Department of Chemical Engineering, Auburn University, Auburn, Alabama, USA selen-cremaschi@auburn.edu

Abstract

Cardiovascular diseases (CVDs) are the number one cause of death worldwide. Mass production of engineered heart tissue using differentiation of human-induced pluripotent stem cells (hiPSCs) can substitute a large number of the lost heart muscle cells in patients with CVDs. However, the scale-up of the differentiation systems for heart tissue, i.e., cardiomyocyte (CM), production is challenging because many parameters affect the process. Machine learning (ML) techniques can be employed to identify critical process parameters for differentiation systems and build models to elucidate the impact of these parameters on process outcomes. Here, we present a ML model to predict CM content on day 10 of the differentiation. Phase-contrast images of microspheroid tissues on differentiation day 5 are the inputs of the ML model, and the output is CM content on 10 of differentiation, classified as either sufficient and insufficient. Support vector machines are used as the classifier models. We utilized feature extraction and selection methods. The best classifier had an accuracy of 77% in predicting the sufficient CM content class.

Keywords: cardiac differentiation, machine learning, support vector machines

1. Introduction

Heart muscle cells (cardiomyocytes (CMs)) are one of the least regenerative cells in the body. Cardiovascular diseases (CVDs) can lead to heart failure and loss of in the order of billion CMs (Kempf et al., 2016). Few viable treatments are present for patients with CVD and post-heart attack problems. Production of CMs via differentiation from human-induced pluripotent stem cells (hiPSCs) may contribute to developing and testing therapeutics for CVDs, e.g., in fields such as drug monitoring and cell therapy (Denning et al., 2016). Mass production of CMs and their implementation in cell therapy of CVD patients is another potential application of hiPSC-derived CMs (hiPSC-CMs).

The production of CMs by differentiation of hiPSCs in a 3D platform is a complex, expensive process, and a high number of parameters impact the system performance (Gaspari et al., 2018). The 3D platforms are promising for the scale-up of CM production, and identifying critical process parameters and their optimal ranges for 3D platforms is the first step towards scale-up. More specifically, distinguishing an unsuccessful batch from a successful one at an earlier time point of the differentiation would significantly reduce the expense and time required for CM production.

In recent years, machine learning (ML) techniques have been successfully used to study complex systems where fundamental understanding is limited. These techniques use

2 S. Mohammadi et al.

information from data sets to infer the relationships between process parameters (inputs) and outcomes (outputs). With the progress in ML algorithms and computational power, many studies exploited the information contained in images to build models to study different systems, such as quantification of CM contraction using image correlation analysis (Kamgoué et al., 2009) and plant disease detection (Vishnoi et al., 2021).

This study investigates the ability to classify CM content on day 10 of hiPSC-laden microspheroid differentiation using images taken on day 5. The CM content is defined as the percentage of the cells which are CMs on the specific differentiation day. We hypothesize that the phase-contrast images of the cells taken during differentiation include information regarding differentiation progress and that a classifier model can capture this information to distinguish batches with sufficient CM content from those with insufficient. Support vector machines are trained using different extracted feature sets of the phase-contrast images to predict the CM content class. The best model had an accuracy of 77% and an MCC of 0.53.

2. Methods and Materials

2.1. Experiments

HiPSCs were encapsulated within PEG-fibrinogen (PF) by using a novel microfluidic system (Tian and Lipke, 2020) in microspheroids with different sizes and axial ratios (AR). After culturing the hiPSC-laden microspheroids in E8 or mTeSR-1 media for 3 days, the CM differentiation is carried out by supplemented CDM3 or RPMI/B27 minus insulin with CHIR on day 0 and IWP2 on days 1 and 3, respectively. Fresh CDM3 was added on days 3, 5, 7, and fresh RPMI/B27 minus insulin media was added on days 1 and 5. Following day 7 or 10, the microspheroids were cultured with RPMI/B27 (Gibco), and the media was exchanged every 3–4 days. (Figure 1). Phase-contrast images were taken throughout the differentiation timeline on days 0, 1, 3, and 5, shown in Figure 1.

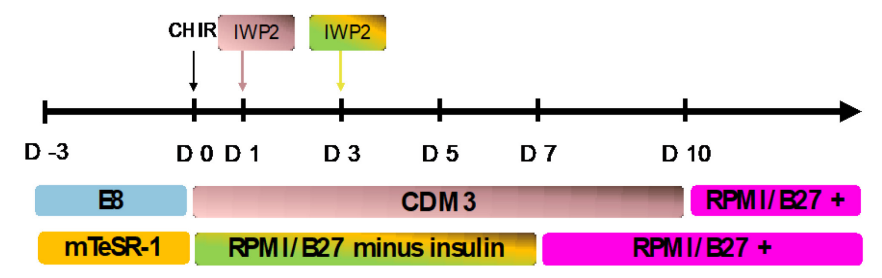


Figure 1. Differentiation protocol of hiPSC-laden microspheroids

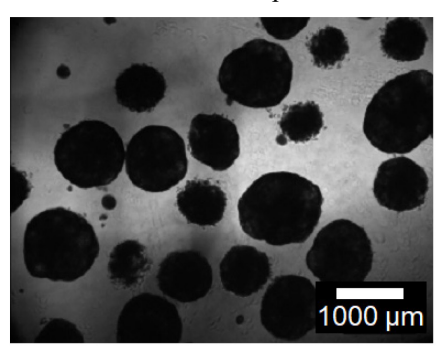
2.2. Data Used to Build the Classifier Model

The initial training data set included 301 phase-contrast images, from day 5 of differentiation, with their corresponding CM content on day 10. Images on day 5 were used because day 5 is the earliest time point without any external stimuli or changes to the system with image availability. Each image contained 496×658 pixels. Figure 2 shows two representative images. The images were augmented to increase the number of training data points to improve the model's generalization. Each image was flipped and rotated (180°) , increasing the number to 903.

CM content above 70% on the 10^{th} differentiation day was defined as the *Sufficient* class, and batched with CM content below 70% belonged to the *Insufficient* class. The data was

Image classification of experimental yields for cardiomyocyte cells differentiated from human induced pluripotent stem cells

split into test and train sets using 20% and 80% of data ratios, respectively. Different classifier models were compared based on their performance on the test set.



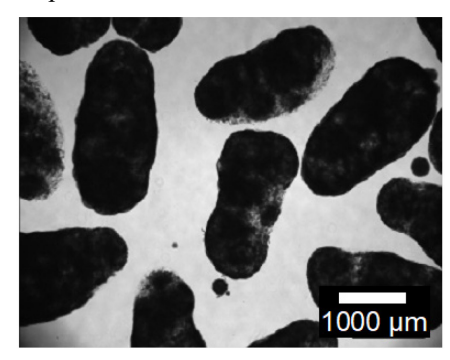


Figure 2. Representative phase-contrast images of microspheroids on day 5

2.3. Feature Extraction

The RGB color space features (color features) of the image pixels formed the initial input feature set. We used two techniques to extract additional features from the images, Histogram of Oriented Gradients (HOGs) (Freeman and Roth, 1994) and texture transformations (Haralick et al., 1973). The HOG feature descriptor is used for object detection and utilizes the local intensity gradient distributions to identify object edges in the images. In the texture transformation method, the grey level co-occurrence matrix (GLCM) is used to calculate six different statistical attributes to explain the image texture patterns. Four different directions, 0°, 90°, 45°, and 135°, were used to calculate the GLCM matrices. The six attributes derived from the co-occurrence matrix (Aborisade et al., 2014; Haralick et al., 1973) includes

1) Contrast, which is a measure of the local intensity variations,

$$Contrast = \sum_{i} \sum_{j} |i - j|^{2} p(i, j)$$
 Eq. 1

2) **Dissimilarity**, which is a localized measure of distance for a pair of pixels,

Dissimilarity =
$$\sum_{i} \sum_{j} |i - j| p(i, j)$$
 Eq. 2

3) **Angular Second Moment (ASM)**, which represents the orderliness of each window of the image,

$$ASM = \sum_{i,j} p(i,j)^2$$
 Eq. 3

4) Energy, which is the square root of the ASM,

$$Energy = \sqrt{ASM}$$
 Eq. 4

5) **Homogeneity**, which represents the local homogeneity within the image by comparing the elements to the diagonal value of the GLCM matrix, and

4 S. Mohammadi et al.

Homogenity =
$$\sum_{i} \sum_{j} \frac{1}{1 + |i - j|^2} p(i, j)$$
 Eq. 5

6) **Correlation**, which is a measure of the linear correlation between the grey-level values of neighbouring pixels.

$$Correlation = \sum_{i} \sum_{j} \frac{(i - \mu_i) (j - \mu_j) p(i, j)}{\sigma_i \sigma_j}$$
 Eq. 6

In Eqs. (1) – (6), p(i, j) is the normalized value of the GLCM matrix element at row i and column j, and μ_i and σ_i are mean and variance for each row of the GLCM matrix components.

We constructed five feature sets as potential inputs for the classifier model using color features, HOG features, and texture transformation features. The first set includes all features (color+HOG+texture), the second color and HOG features (color+HOG), the third color and texture features (color+texture), the fourth HOG and texture features (HOG+texture), and the last one only texture (texture) features. Principal Component Analysis (PCA) (Hotelling, 1933) was used to reduce feature set dimensions. PCA uses orthogonal transformations to build components with a linear combination of the original input features to convert a set of possibly correlated features into uncorrelated ones. The principal components (PCs) explaining 95% of the variance in the input data were considered as classifier inputs.

2.4. Classifier Model Construction and Evaluation

Support Vector Machines (SVMs) (Drucker et al., 2002) were used as the classification models. Linear, radial basis function, and second and third-order polynomials, were evaluated as potential kernels for the SVMs. Kernel selection and regularization parameter tuning were carried out using five-fold cross-validation. Accuracy (Guyon and Elisseeff, 2003), recall (Sokolova and Lapalme, 2009), precision (Sokolova and Lapalme, 2009), and Mathew's correlation coefficient (MCC) (Matthews, 1975) were the metrics used for comparing the performance of the classifiers.

3. Results and Discussion

The performance of classification models in predicting the CM content class for the test points is shown in Figure 3. Figure 3 includes a plot of the performance metrics of the classifiers trained using each feature set. The classifiers were trained using the original data set and the augmented data set, and the performance metrics are plotted separately for these classifiers. The plots only include performance metrics calculated using the test data. Figure 3 reveals that the SVM employing the texture transformation features yielded the best performance with an accuracy of 77%, a recall of 92%, a precision of 75%, and an MCC of 0.53. The data augmentation improved the classifier model performance for the ones employing features other than textures transformations. Because texture features, except for those in which the GLCM matrix was calculated in 45° and 135° directions, are obtained using global transformations, their values are both rotation and flip invariant. As a result, the models that employ texture transformation features perform similarly when trained using the original data set or the augmented one.

The performance of classification models trained using PCs is given in Figure 4. The classifiers that employ the texture features had the best performance with an accuracy of

Image classification of experimental yields for cardiomyocyte cells differentiated from human induced pluripotent stem cells

74% and an MCC of 0.51. The classifier model trained only using HOG and texture features for constructing the PCs, eliminating all color features, had the worst performance with recall, precision, and MCC of zero. Data augmentation, in general, improved the performance of the classifiers that used PCs as input sets. However, the performance metrics of the classifier models using PCs as inputs were lower (worse) than those of classifier models built using raw texture, color, and HOG features.

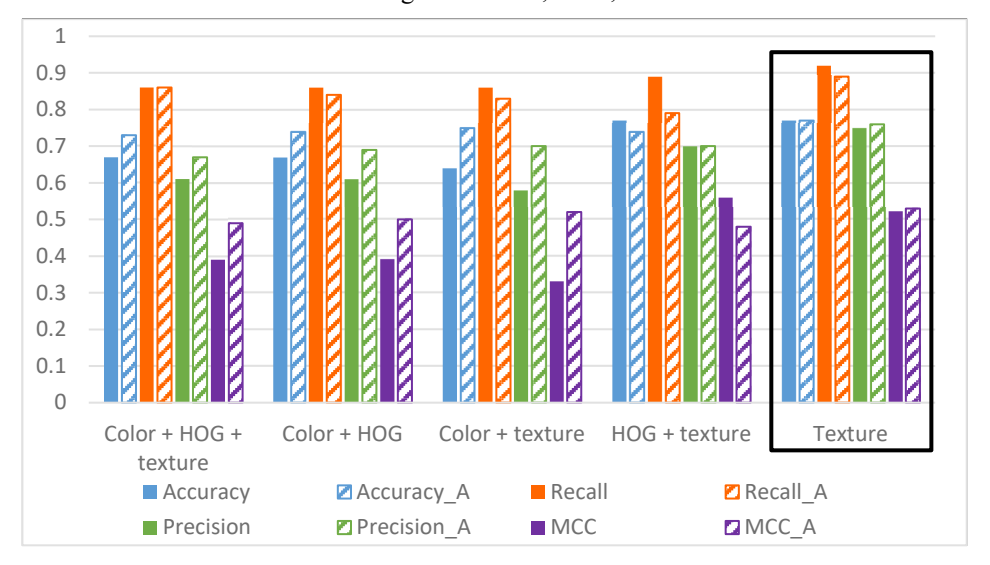


Figure 3. Bar plots of SVM classifier performance metrics trained using different feature sets for the original data set (solid bars) and augmented data set (dashed bars).

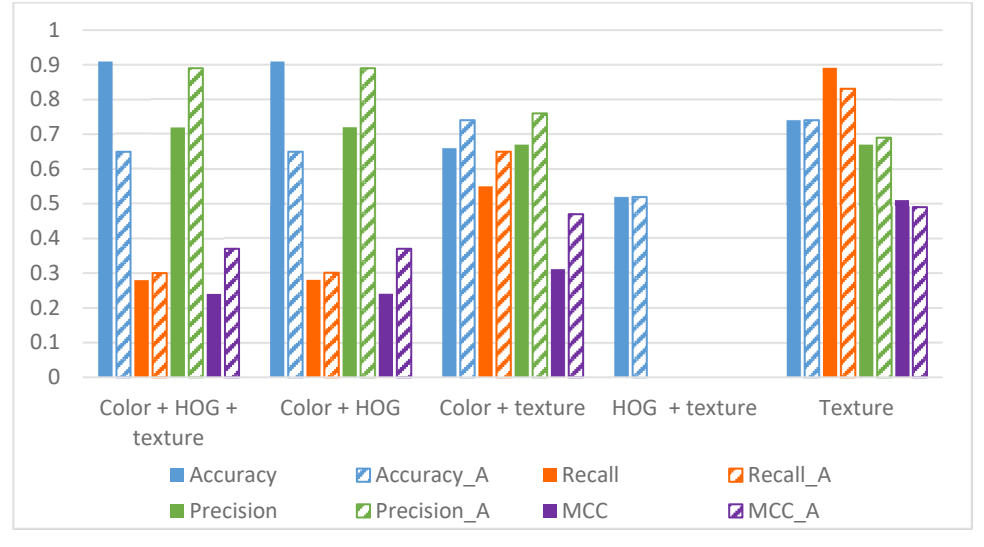


Figure 4. Bar plots of SVM classifier performance metrics trained using PC and different feature sets for the original data set (solid bars) and augmented data set (dashed bars).

6 S. Mohammadi et al.

4. Conclusions

Imaging is commonly used for tracking human induced pluripotent stem cell (hiPSC) differentiation. Using image-based classification, we built binary classification models to predict *Sufficient/Insufficient* classes of cardiomyocyte (CM) content in cells differentiated from hiPSCs. Feature extraction methods were implemented to identify and use the significant features from images to build the classifier. The experimental batched with a CM content above 70% was labeled as the *Sufficient* class, and our classifier was able to predict the classes with 77% accuracy. Future work will include consideration of mixed data from experimental variables and images and consideration of convolutional neural networks as the ML technique to improve the performance of the classifier models.

5. Acknowledgments

This work was funded by NSF grants #1743445 and #2135059.

References

- Aborisade, D.O., Ojo, J.A., Amole, A.O., Durodola, A.O., 2014. Comparative Analysis of Textural Features Derived from GLCM for Ultrasound Liver Image Classification. Int. J. Comput. Trends Technol. 11, 239–244. https://doi.org/10.14445/22312803/ijctt-v11p151
- Drucker, H., Shahrary, B., Gibbon, D.C., 2002. Support vector machines: Relevance feedback and information retrieval. Inf. Process. Manag. 38, 305–323. https://doi.org/10.1016/S0306-4573(01)00037-1
- Freeman, W.T., Roth, M., 1994. Orientation Histograms for Hand Gesture Recognition. Gesture. Gaspari, E., Franke, A., Robles-Diaz, D., Zweigerdt, R., Roeder, I., Zerjatke, T., Kempf, H., 2018. Paracrine mechanisms in early differentiation of human pluripotent stem cells: Insights from a mathematical model. Stem Cell Res. 32, 1–7. https://doi.org/10.1016/j.scr.2018.07.025
- Guyon, I., Elisseeff, A., 2003. An introduction to variable and feature selection. J. Mach. Learn. Res. 3, 1157–1182.
- Haralick, R.M., Shanmugam, K., Dinstein, I., 1973. Textural Features for Image Classification. IEEE Trans. Syst. Man. Cybern. SMC-3, 610–621.
- Hotelling, H., 1933. Analysis of a complex of statistical variables into principal components. J. Educ. Psychol. 24, 417.
- Kamgoué, A., Ohayon, J., Usson, Y., Riou, L., Tracqui, P., 2009. Quantification of cardiomyocyte contraction based on image correlation analysis. Cytom. Part A 75, 298– 308. https://doi.org/10.1002/cyto.a.20700
- Kempf, H., Andree, B., Zweigerdt, R., 2016. Large-scale production of human pluripotent stem cell derived cardiomyocytes. Adv. Drug Deliv. Rev. 96, 18–30. https://doi.org/10.1016/j.addr.2015.11.016
- Matthews, B.W., 1975. Comparison of the predicted and observed secondary structure of T4 phage lysozyme. Biochim. Biophys. Acta Protein Struct. 405, 442–451. https://doi.org/10.1016/0005-2795(75)90109-9
- Sokolova, M., Lapalme, G., 2009. A systematic analysis of performance measures for classification tasks. Inf. Process. Manag. 45, 427–437. https://doi.org/10.1016/j.ipm.2009.03.002
- Tian, Y., Lipke, E.A., 2020. Microfluidic Production of Cell-Laden Microspheroidal Hydrogels with Different Geometric Shapes. ACS Biomater. Sci. Eng. 6, 6435–6444. https://doi.org/10.1021/acsbiomaterials.0c00980
- Vishnoi, V.K., Kumar, K., Kumar, B., 2021. Plant disease detection using computational intelligence and image processing, Journal of Plant Diseases and Protection. Springer Berlin Heidelberg. https://doi.org/10.1007/s41348-020-00368-0